Biochimica et Biophysica Acta, 1058 (1991) 386–399

ADONIS 000527289100174B

BBABIO 43437

Cardiac contractile function, oxygen consumption rate and cytosolic phosphates during inhibition of electron flux by amytal – a ^{31}P-NMR study

V.V. Kupriyanov, V.L. Lakomkin, O.V. Korchazhkina, V.A. Stepanov, A.Ya. Steinschneider and V.I. Kapelko

Institute of Experimental Cardiology, National Cardiology Research Centre, Moscow (U.S.S.R.)

(Received 4 March 1991)

Key words: Amytal; Oxygen consumption; Cardiac contraction; Coronary flow; Isoproterenol; Cytosolic phosphate; NMR, ^{31}P-

In order to investigate the potential role of cytosolic phosphates ([ATP], [ADP] and [P_i]) in the integration of mitochondrial respiration and mechanical function in the perfused heart, inhibition of the substrate end of the respiratory chain by amytal has been employed. A stepwise increase in amytal concentration (from 0.2 to 1.2 mM) resulted in the progressive abolition of the cardiac oxygen consumption, rate (V_{O_2}) in hearts oxidizing pyruvate (5 mM). The inhibition curve for V_{O_2} was S-shaped, with $K_{0.5} = 1.1$ mM, and independent of the initial V_{O_2} values varied by coronary flow and isoproterenol (Iso) addition. ADP-stimulated respiration of isolated mitochondria (malate + pyruvate) was twice as sensitive to amytal inhibition, whereas state 2 respiration (before ADP addition) had the same sensitivity as cardiac V_{O_2}. Decrease in V_{O_2} was followed by a decline in phosphocreatine (PCr) content and augmentation of P_i at nearly constant ATP level and intracellular pH as assessed by the ^{31}P-NMR method. These changes were associated with an elevation of cytosolic free [ADP] and a reduction of the [ATP]/[ADP] ratio and ATP affinity calculated from creatine kinase equilibrium. Concomitantly, pressure-rate product (PRP), maximal rates of contraction and relaxation fell down and the end diastolic pressure (EDP) rose at all initial loads. Amytal-inhibited hearts retained the capability to respond to Iso stimulation (0.1 μM, about 50% enhancement of PRP) even at 1 mM amytal, but their response to elevation of coronary flow was greatly diminished. Alterations in the PRP value induced by the inhibitor at a fixed coronary flow correlated negatively with cytosolic [ADP] and [P_i], and positively with [ATP]/[ADP] and A(ATP). In contrast, EDP correlated with all these parameters in the opposite manner. However, when PRP was varied by coronary flow in the absence of the inhibitor or at its fixed concentrations, such correlations were absent. These data imply that cytosolic phosphates can serve as a feedback between energy production and utilization when the control point(s) is (are) at the mitochondria. In contrast, other regulatory mechanisms should be involved when control is distributed among different steps located both in energy producing and utilizing systems.

Introduction

It is well known that oxygen consumption rate is tightly related to mechanical work performed by cardiac muscle [1–3]. However, the mechanisms providing such effective coordination of these two processes are not completely understood. Among possible mechanisms, sequential feedback control of mitochondrial ATP production and its utilization in myofibrils by

Abbreviations: Iso, isoproterenol; $V_{(O_2)}$, oxygen consumption rate; PRP, pressure-rate product; EDP, end diastolic pressure; Cr, creatine; PCr, phosphocreatine; PP, phosphorylation potential; LV, left ventricular; LVDP, LV developed pressure; HR, heart rate; CF, coronary flow; AN, adenine nucleotide; IAAm, iodoacetamide; DG, deoxyglucose.

Correspondence: V.V. Kupriyanov, Lab. of Bioenergetics, Institute of Experimental Cardiology, National Cardiology Research Centre, 3rd Cherepkovskaya Str., 15A, Moscow, 121552, U.S.S.R.

products and substrates of these reactions, viz., by cytosolic [ATP], [ADP] and [P_i] was considered (Refs. 3–17, for review see Refs. 18–23). Also, participation of phosphocreatine (PCr), creatine (Cr) and creatine kinase isozymes in such control was proposed [18,22,24–28].

Changes in the aforementioned cytosolic parameters related to alterations in cardiac work (and oxygen consumption rate) were usually induced by changing myofibrillar demands in high-energy phosphates or mitochondrial ATP supply, or both [1–3,8–13,15–17]. In particular, mitochondrial ATP production was often controlled by the restriction of oxygen delivery (hypoxia, anoxia) followed by a suppression of contractile function, reduction of the PCr level and cytoplasmic phosphorylation potential (PP) combined with an elevation of cytosolic [ADP] and [P_i] [9,11,15,21]. These data were considered to support the idea on the regulation of contraction by cytosolic phosphates and/or PP [9,11,15,21]. However, cardiac hypoxia is a spatially inhomogenous process due to the heterogeneity of microcirculation and unequal oxygen supply to different zones of the myocardium [29]. Hence, the rate of energy turnover in these zones may be different and, therefore, measured metabolic parameters ([PCr], [ADP], [P_i] and PP) represent the average of their different microscopic values throughout the heart. Inhibitors of the respiratory chain such as amytal may provide a more uniform pattern of distribution of metabolic and physiological parameters due to, presumably, an equal distribution of the inhibitor among the cells (see Refs. 8, 10). Therefore, application of the inhibitor may give more precise relationships between cardiac work, oxygen consumption rate and cytosolic [ADP], [P_i] and PP.

Additionally, amytal known as an inhibitor of NADH-CoQ reductase [7,8], may mimic the regulation of electron flux via the mitochondrial [NADH]/[NAD^+] ratio, that occurs in many cases including Ca^{2+} regulation of pyruvate, isocitrate and 2-oxoglutarate dehydrogenases (PDH, ICDH and OGDH, respectively) [23,30–331. On the other hand, blocking this segment of the respiratory chain may loosen the control exerted by the above-mentioned dehydrogenases.

For these reasons we have investigated the effects of different amytal concentrations on cardiac work, diastolic pressure, oxygen consumption rate (V_{O_2}) and levels of cytosolic phosphates at various coronary flow rates. Data obtained show that cardiac work and V_{O_2} correlate directly with PP and inversely with cytosolic [ADP] and [P_i] when they have been changed by amytal and do not correlate with these parameters when they have been altered by coronary flow variations. These data are discussed in terms of the interplay of sequential (via cytosolic phosphate metabolites) and parallel (via Ca^{2+} regulation) mechanisms of coordination of oxygen consumption and contractile function.

Materials and Methods

Perfusion of isolated rat heart. Hearts of male Wistar rats weighing 250–350 g were perfused by the Langendorff method with P_i-free Krebs-Henseleit buffer. Pyruvate (5 mM), lactate (3 mM) or glucose (11 mM) were used as oxidizable substrates. A water-filled latex balloon was placed in the left ventricular (LV) cavity and the LV pressure was measured by the pressure transducer Gould Statham P23Db and recorded on a Gould 2400 recorder. Hearts were perfused with a constant flow (10–20 ml/min per g wet wt) by a peristaltic pump (Masterflex), the perfusion pressure being 70 to 120 mmHg. The LV diastolic pressure was set at 16–20 mmHg, at which maximal developed pressure was observed. Cardiac work index, pressure-rate product (PRP), was calculated as the product of LV developed pressure (LVDP) and spontaneous heart rate (HR). To introduce the perfused heart into a wide-bore NMR magnet (CXP-200, Bruker), the heart was placed in a rubber sack and completely immersed into the perfusate. The rubber sack with the heart inside was placed in a 20 mm sample tube containing some D_2O and this system was positioned in the NMR magnet (see Refs. 25–27).

Experimental protocol. Two types of experimental protocol were used. First, amytal was added stepwise into the perfusate in increasing concentrations from 0.0 through 0.2, 0.5, 0.8, 1.0 to 1.2 mM at a fixed coronary flow during the experiment. Each step was continued for 10 min, during which time two ^{31}P-NMR spectra were accumulated or oxygen concentration in the effluent was measured at continuous registration of the physiological parameters. Then perfusion was returned to control conditions (no inhibitor) and PRP recovered to approx. 80% of the initial magnitude. Second, the coronary flow was elevated stepwise from 15 through 20 to 25 ml/min (66 ± 1.9, 84 ± 1.9 and 119 ± 4.9 ml/min per g dry wt, respectively) for 10 min at each step (see below). Afterwards, it was reduced to the initial value and 0.2 or 0.5 mM amytal was added and coronary flow steps were repeated with the subsequent washout of the inhibitor during 10 min at minimal coronary flow. Then, a second concentration of amytal was introduced (1.0 or 1.5 mM, correspondingly) and steps of the coronary flow were repeated again and followed by inhibitor washout. This protocol is presented below:

Coronary flow (ml/min)	15	20	25	15	15	20	25	15	15	20	25	15
Time interval (min)	10	10	10	10	10	10	10	10	10	10	10	10
[amytal] (mM)	0	0	0	0	0.2 (0.5)	0	1.0 (1.5)	0				

Both of these approaches gave similar results.

NMR experiments. ^{31}P-NMR spectra of perfused hearts were usually accumulated each 5 min at a standard frequency of 80.98 MHz by applying 90 degree sampling pulses with a 2 s repetition time. Each spectrum was obtained by the collection of 150 transients in a 4K memory block, the resulting signal was exponentially multiplied with a line broadening factor of 10–20 Hz and was Fourier transformed yielding a frequency spectrum in the 4000 Hz (50 ppm) spectral range.

To suppress spin–spin interaction (^{1}H–^{31}P) broadband proton decoupling (0.2 wt) was used over the period of the spectrum acquisition. At the beginning and at the end of the experiment, quantitative spectra with a 10 s repetition time (90 acquisitions) were accumulated. Peak areas at cut-off from these spectra were used to calculate the tissue content of PCr, ATP and P_i. The peak of methylene diphosphonate (10 μmol of ^{31}P) was used as a reference for spectra quantitation. Solution of this compound (100 mM) sealed in a plastic tube was placed in the vicinity of the heart.

Isolation of mitochondria. Mitochondria were isolated from rat hearts by the trypsin digestion method [34] in a medium containing 0.3 M sucrose, 10 mM Hepes-K (pH 7.2), 0.2 mM EDTA and 1 mg/ml bovine serum albumin. Mitochondrial preparations were suspended in isolation medium. They exhibited state 3 respiration rates of 438 ± 56 ng atoms of O_2/min mg and an acceptor control index of about 6 with pyruvate plus malate as oxidizable substrates at 36 °C and pH 7.2.

Measurements of oxygen consumption in isolated heart and mitochondria. The oxygen consumption rate by perfused heart was determined as the difference in oxygen concentrations between aortic inflow and pulmonary artery outflow perfusate multiplied by coronary flow rate. A Clark-type oxygen electrode and a Beckman oxygen analyzer were used for permanent monitoring of the oxygen concentration in the perfusate.

Respiration of isolated mitochondria was determined using a Yellow Spring Clark electrode assembly in a medium containing 0.25 M sucrose, 20 mM Hepes-K (pH 7.2 or 7.4), 5 mM pyruvate, 2 mM malate, 3 mM magnesium acetate, 4 mM potassium phosphate, 2 mM EDTA, 0.3 mM EGTA, 1 mg/ml bovine serum albumin and 0.3 mM dithiothreitol at 36°C. The mitochondrial concentration was about 1 mg/ml and ADP, 0.1 mM.

Biochemical assays. Hearts were frozen in liquid nitrogen by Wollenberger clamps. Frozen tissue was pulverized in a mortar and extracted by 6% perchloric acid. Neutralized extracts were used for the spectrophotometric enzymatic measurements of ATP, ADP, AMP and PCr according to Bergmeyer [35] and for the colorimetric assay of total and free creatine [36].

Calculations of cytosolic [ADP], [ATP] / [ADP] and ΔG[ATP]. All these parameters were calculated from creatine kinase equilibrium:

$$[ATP]/[ADP] = K_{eq}[PCr]/[Cr]$$

The constant of equilibrium for creatine kinase reaction, K_{eq} was taken to be 104 assuming an intracellular $[Mg^{2+}]$ of 1 mM and pH 7.2 [37]. PCr content was determined from ^{31}P-NMR spectra and the Cr content was calculated as a difference between total Cr and PCr contents. In order to determine the concentrations of cytosolic phosphates, the cytoplasmic water content was estimated as 2.5 ml/g dry wt. [38]. P_i determined from NMR spectra at 4.95 ppm downfield of the PCr peak was considered as cytosolic and, therefore, its concentration in mM was obtained by dividing the P_i content in μmol/g dry wt. by a factor of 2.5. Assuming that mitochondrial ATP is NMR-visible, the mitochondrial pool of adenine nucleotides (AN) is 20% of total [39] and intramitochondrial [ATP]/[ADP] = 3 [40], the ATP content was taken to be 15% of the total and was subtracted from the total to estimate the cytoplasmic content. The latter was divided by a factor of 2.5, thereby giving the cytosolic ATP concentration which was used for the calculation of cytosolic [ADP] according to the formulae presented above. Finally, affinity for ATP, A(ATP), and free energy of ATP hydrolysis, G(ATP) were determined from the [ATP]/[ADP] ratio and cytosolic $[P_i]$ using the following equation:

$$A(ATP) = -\Delta G(ATP) = \Delta G_0 - 2.3RT \log[ATP]/[ADP]\cdot[P_i]$$

where $\Delta G_0 = -30.5$ kJ/mol [15,20].

Reagents. Enzymes, nucleotides, Hepes, EDTA, EGTA, creatine, sodium pyruvate, sucrose, dithiothreitol, bovine serum albumin and trypsin were obtained from Sigma (U.S.A.) or Serva (F.R.G.). Sodium amytal was purchased from Serva. Salts were purest and analytical grades.

Results

Oxygen consumption rates

Fig. 1 shows the inhibition of cardiac oxygen consumption by amytal at three different initial loads produced by coronary flow (CF) elevation (from 67 to 87 ml/min per g dry wt) and by isoproterenol addition (Iso, 0.1 μM, CF-88 ml/min per g dry wt). It is seen that all inhibition curves were S-shaped, i.e., a minimal inhibitor concentration did not affect V_{O_2}. When these data were normalized to the initial V_{O_2} values all three curves were transformed into one curve with $K_{0.5}$ for amytal about 1.1 mM. This value is close to that found for this inhibitor in glucose perfused rat hearts [8,10]. It is interesting that ADP-stimulated (100 μM) state 3 respiration of isolated heart mitochondria oxidizing mixture of pyruvate plus malate was much more sensi-

tive ($K_{0.5}$ = 0.47 mM) to amytal inhibition (Fig. 1B). However, the inhibition curve for state 2 respiration (before ADP addition) when the electron flux was controlled by energy dissipation was close to that for cardiac oxygen consumption (Fig. 1B). In order to analyze the control points of cardiac respiration, relative values of oxygen consumption rates ($V_{O_2}/V_{O_2(0)}$) were plotted against the degree of inhibition of mitochondrial respiration by amytal (Fig. 1C). These curves are inflected upward and, therefore, are much above the dotted straight line connecting the maximal axis points. This straight line corresponds to the case of identity of inhibition curves for respiration of the heart and isolated mitochondria. If in isolated mitochondria in the presence of excess of ADP and oxygen, the NADH-CoQ reductase segment (Complex I) of the respiratory chain is the only control point, then a degree of inhibition reflects the relative content of inactive (inhibited) Complex I. Therefore, the aforementioned straight line corresponds to hypothetical situation of absolute control (control strength [40,41], CS = 1.0) of cardiac respiration at the Complex I level and experimental curves do to some intermediate case (CS < 1.0). The apparent control strength value can be roughly estimated as 0.35. This value is certainly overestimated, since amytal is not an irreversible inhibitor and also the substrate regulation of NADH-dehydrogenase by NADH and NAD^+ complicates careful analysis.

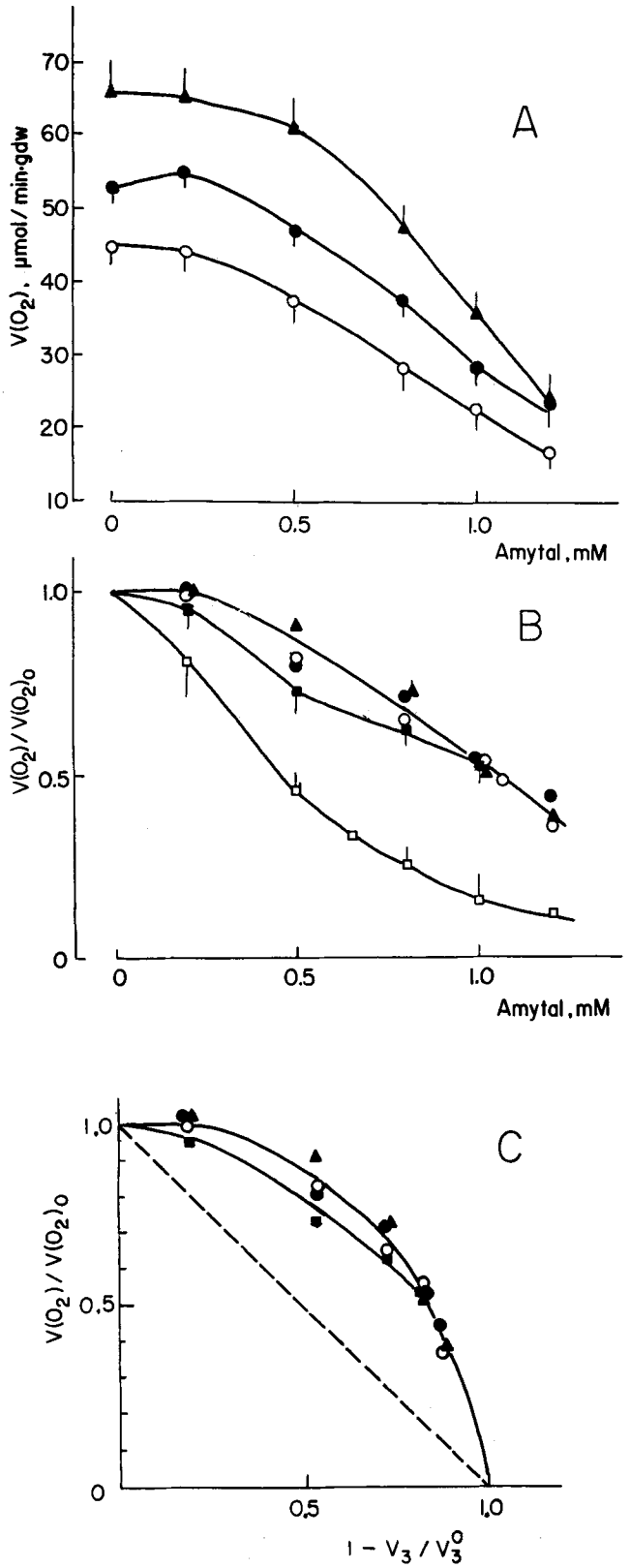

Functional effects

Fig. 2A–D demonstrates the effect of amytal at different initial loads produced by coronary flow variations and by Iso administration on the functional parameters of isovolumic rat hearts perfused with pyruvate. It is seen that amytal suppresses PRP by 50% in concentrations ranging from 0.5 to 0.8 mM. The same inhibition pattern was observed when lactate (3 mM) was used as a sole exogenous substrate at minimal coronary flow (not shown). It is interesting that the sensitivity to inhibition is somewhat higher at higher workloads produced by elevation of coronary flow. However, at maximal workload produced by isoproterenol stimulation (CF = 90 ml/min per g dry wt) the sensitivity to amytal inhibition is similar to that at minimal work. Amytal in any concentration almost

Fig. 1. Inhibition of oxygen consumption rate by amytal in perfused heart and isolated mitochondria. (A) V_{O_2} versus amytal concentration; (B) Relative values of oxygen consumption rates, $V_{O_2}/V_{O_2(0)}$, as functions of amytal concentration. Current magnitude of parameter, V_{O_2}, is divided by the initial one, $V_{O_2(0)}$, for each experimental series. See explanation in the text., C.Dependence of relative value of cardiac oxygen consumption rate (V/V_0) on degree of inhibition of mitochondrial state 3 respiration (V_3/V_3^0). V_3 and V_3^0 are respiration rates in the state 3 in the presence and in the absence of amytal, respectively. Keys: perfused heart: coronary flow in ml/min per g dry wt: ○, 64±2.5; ●, 82±2; ▲, 82±8.3 plus 0.1 μM Iso; isolated mitochondria: □, state 3 respiration in the presence of 100 μM ADP, V_3^0 = 438±56 ng-atom/min per mg; ■, state 2, no ADP, V_0 = 71±6 ng atom/min per mg.

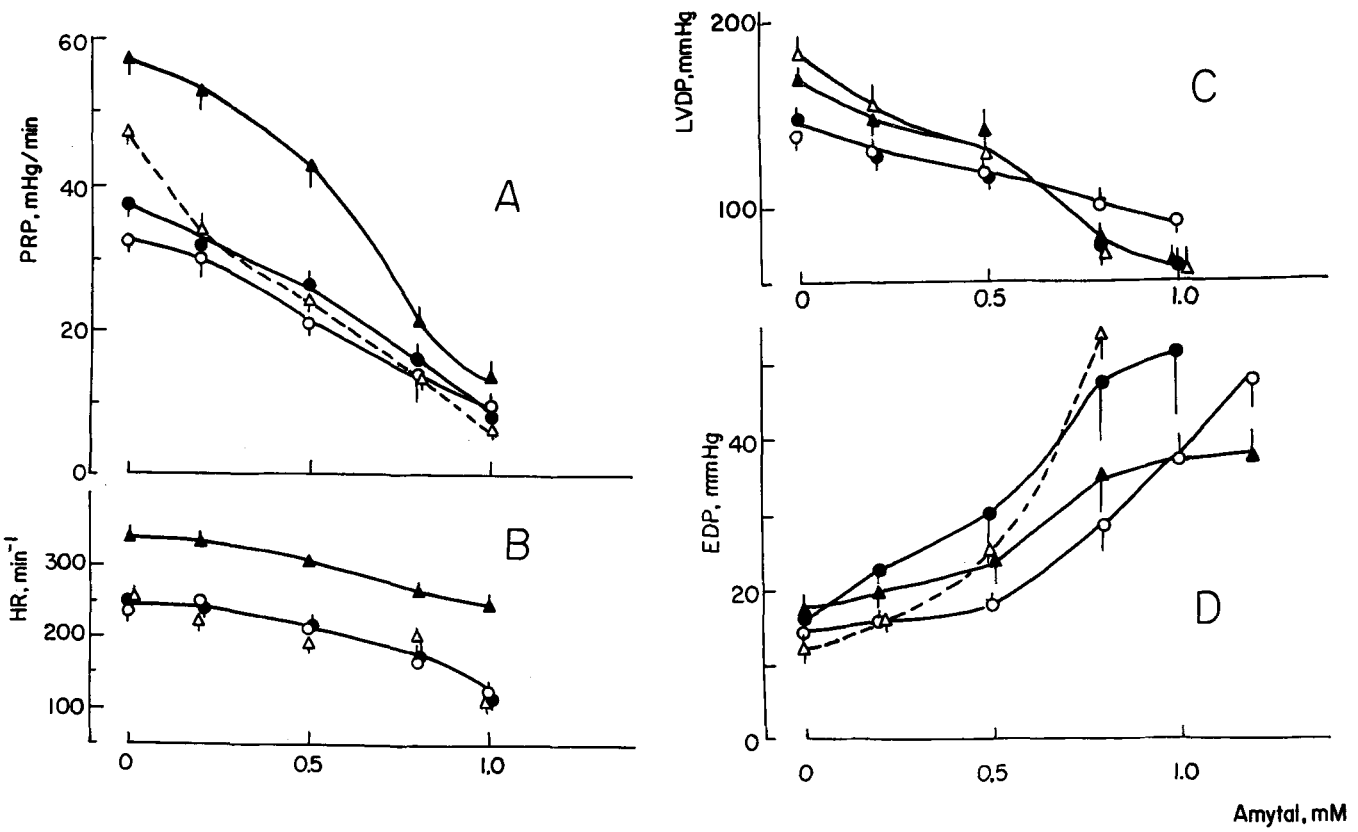

Fig. 2. The effect of amytal on functional parameters of Langendorff-perfused hearts. (A) PRP, pressure-rate product is heart rate×LV developed pressure. (B) HR, heart rate; (C) LVDP, left ventricular developed pressure is the difference between LV systolic and end diastolic pressures; (D) EDP, end diastolic pressure. Means±S.E. for 15 hearts are given. Keys: coronary flow in ml/min per g dry wt. ○, 66±1.9; ●, 84±1.9; △, 119±4.9; ▲, 88±5.2 plus 0.1 μM Iso.

completely abolished cardiac response to coronary flow rise (Fig. 2), whereas the stimulatory effect of Iso remained unchanged (from 51 to 64%).

The amytal-induced reduction of cardiac work is determined by both the decrease in heart rate (HR) and the left ventricular developed pressure (LVDP, Fig. 2B and C). The former was not affected in practice up to 0.5 mM amytal, the latter decreased monotonically in the entire range of the inhibitor concentrations due to both a drop of LV systolic pressure (LVSP, not shown) and an elevation of end diastolic pressure (EDP) (Fig. 2D). Again, the changes were more pronounced at higher coronary flows and higher amytal concentrations. Also, amytal caused some decrease in perfusion pressure (by 15%), most probably due to the known amytal-induced vasodilating effect [7,8,10] and constant coronary flow maintained by peristaltic pump. However, this decrease in perfusion pressure is too small to contribute markedly to observed reduction in cardiac work. Besides, a decrease in PRP value cannot be attributed to the inhibition of the conducting system, since under conditions of pacing the sensitivity of the energy turnover rate (V_{O_2}) to amytal inhibition was the same [8,10] as in spontaneously beating hearts in our experiments.

Finally, dependence of the maximal rate of contraction ($+dP/dt_m$) on amytal concentration was similar to that for LVDP, whereas maximal rate of relaxation ($-dP/dt_m$) decreased less than LVDP (except Iso addition) (not shown).

Relationships between V_{O_2} and PRP

Cardiac oxygen consumption rate was linearly related to PRP magnitude regardless whether they were varied by amytal or coronary flow (Fig. 3). Fig. 3A represents correlations of V_{O_2} with PRP grouped according to coronary flow rates so that changes in V_{O_2} and PRP within each line were due to amytal inhibition. One can see that the slopes of the straight lines became lesser and the ordinate intercepts corresponding to zero workload became greater (from 12 to 25 μmol/min per g dry wt) as coronary flow rose or Iso was added (Fig. 3A). This implies that a unit of mechanical work requires less amounts of oxygen at higher flows or in the presence of Iso, while the amounts of oxygen necessary for other cellular functions (e.g., ionic pumping) tend to be higher under these conditions. Note, however, that the line showing a relationship between PRP and V_{O_2} in the presence of Iso is broken and can be approximated by two linear parts. Also, all

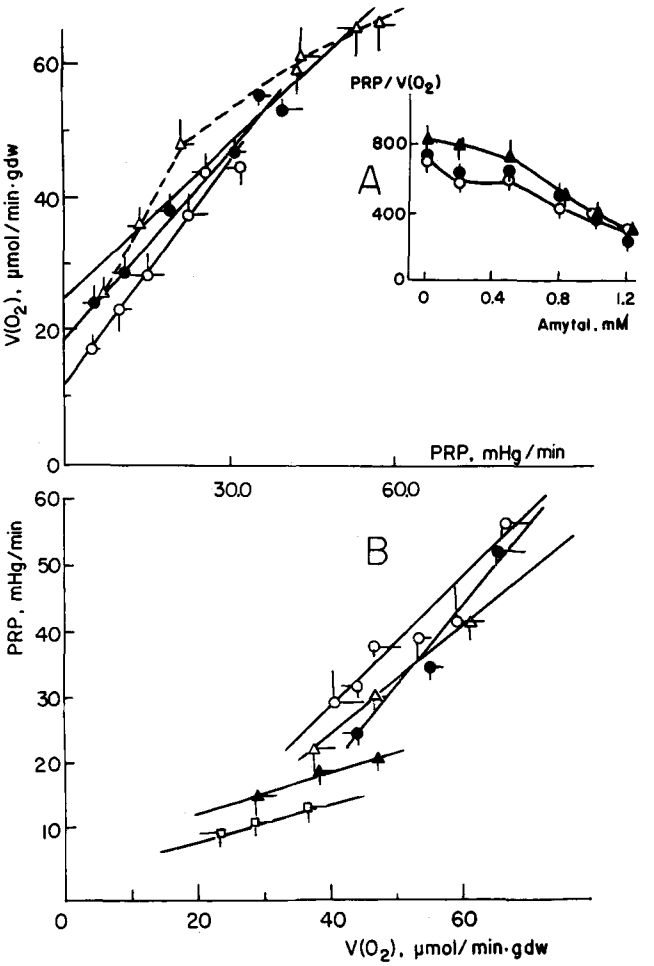

Fig. 3. Dependence of oxygen consumption rate on cardiac work index (PRP) in perfused rat heart. (A) Straight lines are plotted in accordance with coronary flow rates in ml/min per g dry wt: ○, 64±2.5; ●, 82±2; ▲, 82±8.3 plus Iso. These straight lines are approximated by equations: $y = 1.08x + 12.5$ ($r = 0.99$); $y = 0.92x \pm 19.2$ ($r = 0.99$); $y = 0.77x + 25.4$ ($r = 0.97$), respectively. Within each curve the decrease in PRP and V_{O_2} was due to elevation of amytal concentration. Insert: PRP values are referred to V_{O_2}. (B) Straight lines correspond to fixed inhibitor concentrations in mM: ○, 0.0; ●, 0.2; △, 0.5; ▲, 0.8; □, 1.0. Slopes of the lines are 0.95 ($r = 0.95$), 1.33 ($r = 0.98$), 0.83 ($r = 1.0$), 0.33 ($r = 0.98$), 0.31 ($r = 0.999$), respectively. Within each curve the increase in PRP and V_{O_2} was due to elevation of coronary flow and Iso addition (maximal points).

these data were divided in groups corresponding to different inhibitor concentrations when changes in PRP and V_{O_2} within each line were induced by coronary flow variations (Fig. 3B). Again, it is a set of straight lines, the slopes of which are different; they are high at low amytal concentrations (0.0–0.5 mM) and small at high inhibitor concentrations (> 0.8 mM). This implies that the apparent efficiency of energy utilization for mechanical work ($\Delta PRP/\Delta V_{O_2}$) falls (from 1000 to 120 mmHg/µmol) as the amytal concentration rises. The same is demonstrated by plotting the PRP/V_{O_2} ratio against amytal concentration (inset in Fig. 3A).

Changes in cytoplasmic concentrations of free PCr, P_i, ADP and [ATP] / [ADP) ratio and A(ATP)

Fig. 4 shows changes in representative ^{31}P-NMR spectra of perfused heart induced by amytal which reveal a decrease in PCr and an increase in P_i contents at nearly constant ATP. The average PCr concentration dropped from 14–16 mM to 7.5–9.0 as the amytal concentration rose to 1.0 mM; the curves for all coronary flows were very close (Fig. 5A). However, in the presence of isoproterenol, PCr dropped even more (up to 5 mM at 0.8 mM amytal). Meanwhile, [P_i] rose steadily, reaching maximally 2.5–4.5-times higher values at different coronary flows (Fig. 5B). Note that the position of the P_i peak was not affected or was slightly shifted downfield by approx. 0.08 ppm at minimal CF both in pyruvate and lactate perfused hearts, which indicates a constancy of intracellular pH or a slight alkalization by 0.08 ± 0.01 pH units, respectively. Isoproterenol doubled initial (prior amytal addition) level of P_i and potentiated an amytal-induced rise of P_i.

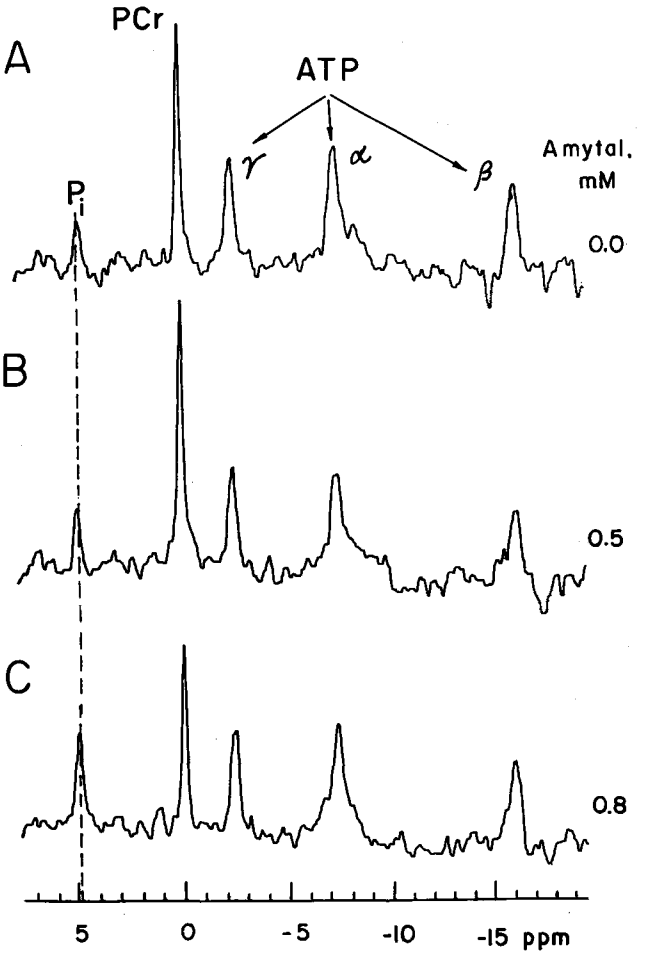

Fig. 4. Effect of amytal on representative ^{31}P-NMR spectra of perfused rat heart. Repetition time, 2 s; number of acquisitions, 150. All spectra were normalized to the reference peak, methylene diphosphonate (19.7 ppm), which is not shown. Wet weight of the heart was 0.85 g.

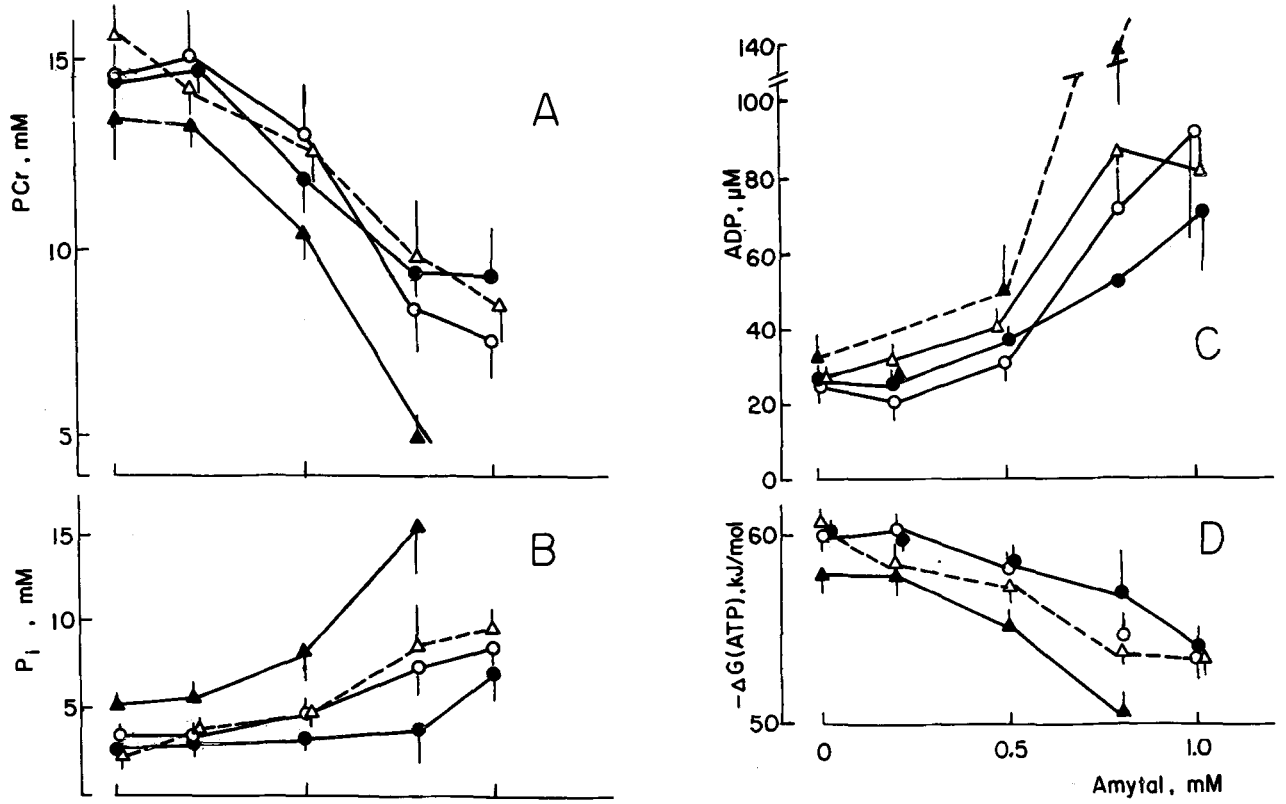

Fig. 5. Changes in the level of phosphates in perfused hearts induced by amytal. (A) PCr, phosphocreatine; (B) P_i, inorganic phosphate; (C) Cytosolic ADP; (D) Free energy of cytosolic ATP hydrolysis, ΔG(ATP). Keys: coronary flow in ml/min per g dry wt.: ○, 70±2.7; ●, 89±2.9; △, 124±5.6 ▲, 97±7.9 plus 0.1 μM Iso. [ADP] and ΔG(ATP) were calculated as described in Materials and Methods.

ATP content reduced slightly (by 20%) due to some loss of the adenine nucleotide (AN) pool induced by prolonged perfusion (about 60 min) in the presence of increasing concentrations of amytal (not shown).

It is interesting that amytal-induced changes in [PCr] and [P_i] were more significant than those observed earlier in hearts perfused with glucose at a constant pressure [10]. This can be explained by the fact that in the cited paper changes in [PCr] and [P_i] could be compensated for activation of glycolysis and coronary flow elevation due to vasodilation [10].

Cytosolic ADP concentration, [ATP]/[ADP] ratio and free energy of ATP hydrolysis (ΔG(ATP)) were calculated from these data on the basis of creatine kinase equilibrium (for details see Materials and Methods). As seen in Fig. 5C, cytosolic ADP increased from 25 μM to 70–90 μM as amytal increased at all coronary flows. In the presence of isoproterenol the curve for [ADP] was systematically shifted upward (except the 0.2 mM point). Naturally, the [ATP]/[ADP] ratio decreased (not shown) reaching values 2.5–3.5-times lower than the initial (Table I) because ATP remained nearly constant; dependencies were very similar for all coronary flows. The only exception is the isoproterenol group, where [ATP]/[ADP] declined 6-fold at 0.8 mM amytal. Finally, the simultaneous reduction of [ATP]/[ADP] and elevation of [P_i] caused a decline in ΔG(ATP) (Fig. 5D), maximally by 6 to 7.5 kJ/mol. Again, the course of these dependencies was very similar for all coronary flows except that for Iso-stimu-

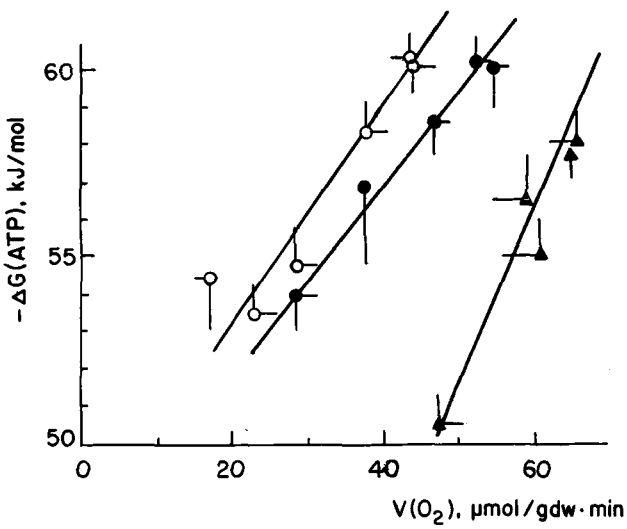

Fig. 6. Dependence of free energy of cytosolic ATP hydrolysis (affinity) on the rate of oxygen consumption in perfused heart. Keys: coronary flow in ml/min per g dry wt.: ○, 64±2.5; ●, 82±2.0; ▲, 82±8.9 plus 0.1 μM Iso. Slopes of the straight lines are 0.25 (r = 0.95), 0.23 (r = 0.99) and 0.40 (r = 0.97), respectively. ΔG(ATP) was calculated as described in Materials and Methods.

TABLE I

The effect of coronary flow on physiological and biochemical parameters of perfused heart

Means ± S.E. are given for 5–15 experiments. Coronary flow (CF) was varied by a peristaltic pump so that each coronary flow step continued for 10 min. Two ^{31}P-NMR spectra were accumulated during this time interval for each coronary flow step and second spectra (between 5 and 10 min) were used for determinations of [PCr], [P_i] and [ATP]. ADP concentration, [ATP]/[ADP] and ΔG(ATP) were calculated from creatine kinase equilibrium as outlined in Materials and Methods. Tissue oxygen consumption rate was measured in separate experiments performed according to the same protocol (see Materials and Methods). Physiological data obtained in both experimental series were pooled for calculations of mean values. Isoproterenol concentration was 0.1 μM. Abbreviations: CF, coronary flow; PRP, pressure-rate product; EDP, end diastolic pressure. Differences between V_{O_2} and PRP values are statistically significant ($P < 0.05$) and those in all other parameters are insignificant.

Parameter CF (ml/min per g dry wt.)	V_{O_2} (μmol min^{-1} g dry wt^{-1})	PRP (mHg) min^{-1})	EDP (mmHg)	PCr (mM)	P_i (mM)	ADP (μM)	[ATP]/[ADP]	$-\Delta G$(ATP) (kJ/mol)
66.2 ± 1.9	44.3 ± 2.7	32.4 ± 1.5	14.5 ± 1.1	14.6 ± 1.0	3.1 ± 0.58	25.2 ± 3.6	237 ± 29	60.0 ± 0.7
88 ± 1.9	52.8 ± 1.6	37.7 ± 2.1	16.4 ± 1.3	14.5 ± 0.9	2.52 ± 0.4	26.4 ± 2.8	214 ± 24	60.2 ± 0.6
119 ± 4.9	n.d	47.3 ± 2.2	12.4 ± 1.4	15.6 ± 0.72	2.22 ± 0.29	25.6 ± 2.4	288 ± 46	60.8 ± 0.4
88 ± 5.2 + Iso	66.2 ± 4.1	57.1 ± 2.2	17.2 ± 2.2	13.4 ± 1.0	4.85 ± 0.72	32.4 ± 6.4	209 ± 32	58.0 ± 0.7

lated hearts, in which A(ATP) was systematically lower at all inhibitor concentrations.

Thus, the inhibition of the respiratory chain at the level of Complex I resulted in a decrease in [PCr], [ATP]/[ADP], A(ATP) and augmentation of [P_i] and [ADP] at a nearly constant ATP level and intracellular

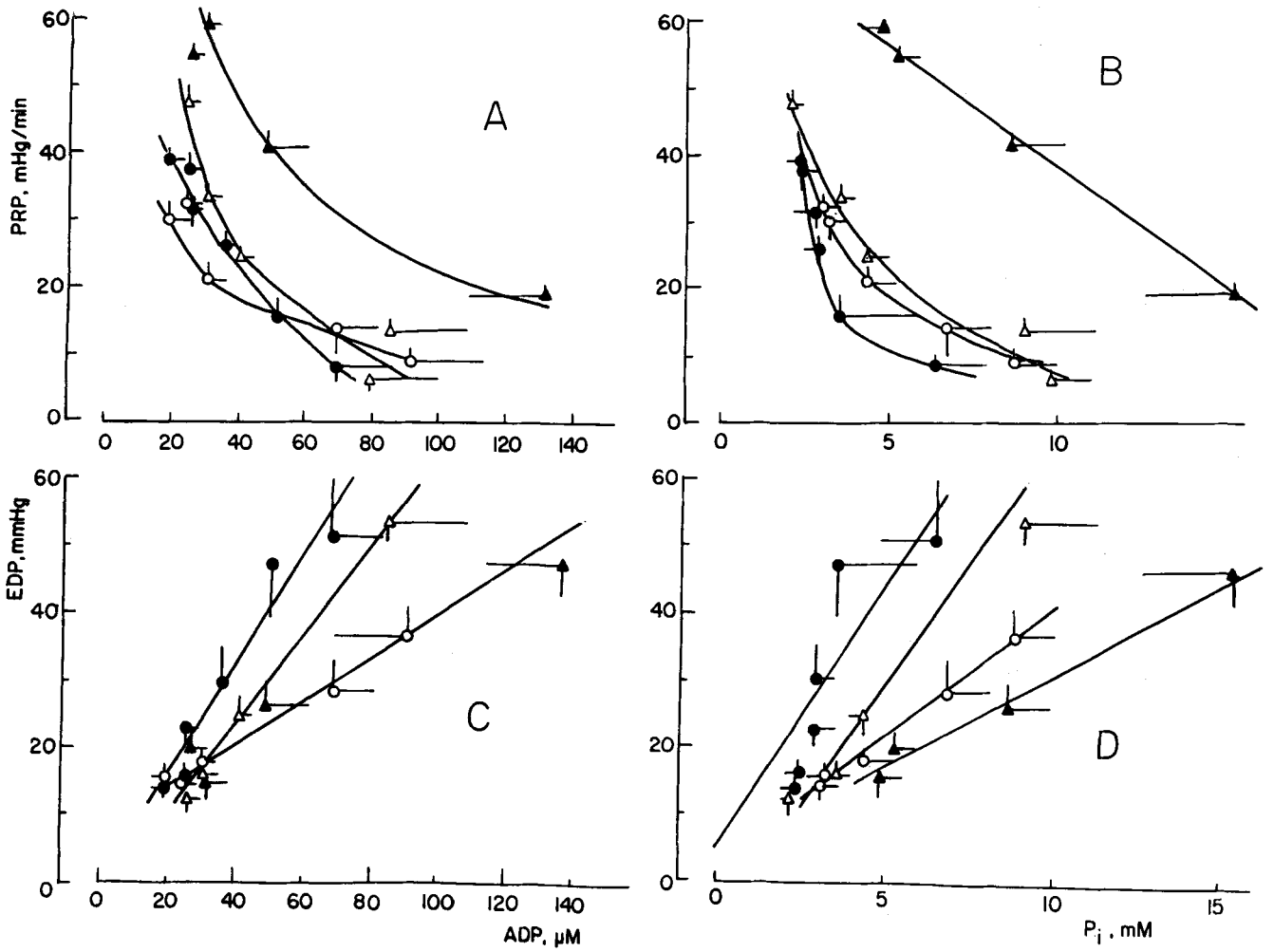

Fig. 7. Correlations of cardiac work index (A,B) and end diastolic pressure (C,D) with cytosolic [ADP] (A,C) and [P_i] (B,D). Data were taken from Figs. 1 and 5. Keys: coronary flow in ml/min per g dry wt: ○, 66 ± 1.9; ●, 84 ± 1.9; △, 119 ± 4.9; ▲, 88 ± 5.2 plus 0.1 μM Iso. Slopes of the straight lines are: (C) 0.30 ($r = 0.99$), 0.78 ($r = 0.96$), 0.68 ($r = 0.999$), 0.27 ($r = 0.98$); (D) 3.85 ($r = 0.99$), 7.66 ($r = 0.81$), 7.24 ($r = 0.985$) 2.86 ($r = 0.995$), respectively. [ADP] was calculated as described in Materials and Methods.

pH. These effects were independent of coronary flow rate but were more profound in the presence of isoproterenol.

Relationships between energy turnover and cytoplasmic phosphate metabolites

Fig. 6 shows the dependence of cytosolic ATP affinity ($A(ATP) = -\Delta G(ATP)$) on the oxygen consumption rate when varying the amytal concentration. A parallel and almost linear fall of $A(ATP)$ from 60 to 53 kJ/mol was observed as V_{O_2} decreased from 55 to 20 μmol/min per g dry wt. at two different coronary flows (66 and 88 ml/min per g dry wt). Iso shifted this dependence to the right and it became steeper. In other words, the same electron fluxes through the respiratory chain and, presumably, rates of mitochondrial ATP synthesis generated significantly lower absolute values of $A(ATP)$ (maximally by 7.5 kJ/mol). It can be explained by much higher demands of myofibrils in energy in the presence of Iso as compared with energy supply.

PRP correlated negatively with [ADP] and [P_i] (Fig. 7A,B) and positively with [ATP]/[ADP] and $A(ATP)$ (not shown) and was not uniformly related to most of these metabolic parameters, since curves corresponding to different coronary flows were not identical (Fig. 7). It is especially pronounced at low [ADP] and [P_i] (high $A(ATP)$ in the absence of amytal (see also Table I). Thus, [ADP] and P_i as well as [ATP]/[ADP] and $A(ATP)$ do not seem to be universal determinants of PRP and, therefore, some other factors connected with coronary flow have to be taken into account. This finding is strengthened by results obtained in the experiments with Iso-stimulated hearts. The respective curves for them were significantly shifted upward for all correlations (Fig. 7A,D). In this case Iso-induced acceleration of Ca^{2+} turnover, perhaps, overcomes inhibition of cardiac work exerted by increased cytoplasmic [ADP] and [P_i].

EDP correlated with metabolic parameters listed above in the opposite manner as compared with PRP (Fig. 7C,D). The former rose linearly as [ADP] (Fig. 7C) or [P_i] (Fig. 7D) increased; each coronary flow was characterized by a distinct individual straight line. Obviously, this means that elevation of EDP was also related to a decrease in [ATP]/[ADP] and $-\Delta G(ATP)$, since ATP remained nearly constant. Two common features of all these correlations are seen. First, data points are concentrated at minimal values of [ADP] and [P_i] (maximal ones of [ATP]/[ADP] and $-\Delta G(ATP)$; no amytal) due to independence of EDP and the listed metabolic parameters on coronary flow rates (see Table I). Second, the correlation lines are steeper at higher coronary flows due to greater EDP values for the same magnitudes of metabolic variable. In the presence of Iso these lines are shifted downward with respect to those for the same coronary flow (88 ml/min g dry wt) and are close to those for minimal coronary flow (Fig. 7C,D). Again, these observations clearly demonstrate that EDP, like PRP, is not only controlled by cytoplasmic phosphates but is also affected by some other factors which are dependent on coronary flow and Iso.

Discussion

Control of cardiac respiration at the Complex I level

Inhibition pattern by amytal was independent of the initial workload and V_{O_2} (see Fig. 1). This means that the degree of control of respiration exhibited by NADH-CoQ reductase is constant at different fluxes through the respiratory chain. There are at least two factors which could partially compensate for the inhibitory effect of amytal. First, the rise of inhibitor concentration or the rate of NADH generation (e.g., due to Iso addition) should facilitate the establishment of a higher [NADH]/[NAD^+] ratio and, therefore, provide some counteraction to the inhibition by amytal. Second, the enhancement of cytosolic [ADP] and [P_i] should result in the activation of the AN translocator and P_i carrier, thereby reducing control at these sites. In other words, it facilitates electron transfer through the respiratory chain behind Complex I, providing something like a 'suction-out' effect. This importance of a control mechanism at the level of AN translocase (and, perhaps, ATP synthase) is seen from the comparison of the inhibition curves for tissue respiration and that of isolated mitochondria (Fig. 1B). Stimulated by the excess of ADP the mitochondrial respiration (state 3) was 2-times more sensitive to amytal than tissue respiration whereas state 2 respiration was as sensitive as the tissue one. This may mean that when electron transfer is not controlled by ADP (state 3) the major control point seems to be at NADH-CoQ reductase due to amytal inhibition. In contrast, at a high cytosolic [ATP]/[ADP] ratio (order of 100) translocase (and ATP synthase) may play a significant role in the control of respiration. Similarly, when respiration is controlled by energy dissipation (state 2) due to H^+ leakage, the NADH-CoQ segment becomes less prominent in the regulation of electron flux. From this viewpoint, an increase in [ADP] and [P_i] in response to Complex I inhibition means loosening the control exerted by these metabolites as a result of the increased control at the level NADH-CoQ reductase. Similar relationships were observed during transition from one oxidizable substrate to another (e.g., from pyruvate to glucose) [17] and during deactivation of PDH by the restriction of Ca^{2+} availability [23,32]. In other words, using terminology by From et al. [17] a transition from an ADP- and P_i-limited domain to an NADH dehydrogenase-limited one takes place.

However, there are other possible reasons for the

different sensitivity of respiration to amytal in tissue and isolated mitochondria. First, the NADH formed during metabolism of pyruvate in the Krebs cycle could be oxidized not only via NADH-dehydrogenase but also by an excess of cytosolic pyruvate (5 mM) in the lactate dehydrogenase reaction. In fact, inhibition of NADH-CoQ reductase by amytal should lead to an elevation of the matrix [NADH]/[NAD^+] ratio and via the malate-aspartate shuttle to an elevation of cytosolic [NADH]/[NAD^+] that may shift the lactate dehydrogenase equilibrium towards pyruvate reduction to lactate. Therefore, the Krebs cycle could function and conversion of succinyl-CoA to fumarate (via the succinate dehydrogenase reaction) proceed with formation of three ATP molecules (2ATP + GTP). However, we have found that in pyruvate perfused hearts the rate of lactate extrusion in the perfusate was similar (about 4 μmol/min per g dry wt) at any amytal concentration, unlike glucose perfused hearts [10]. Also amytal equally suppressed contractile function in pyruvate and lactate perfused hearts. These findings imply that for some reasons mitochondrial NADH cannot be oxidized by cytosolic pyruvate. Also, formation of additional pyruvate from glycogen when lactate is the sole exogenous substrate seems to be impossible, as the rate of pyruvate release into the perfusate was not affected by amytal. This observation is consistent with the absence of acidification of intracellular medium when pyruvate or lactate were oxidizable substrates. Thus, the possible oxidation of NADH by cytosolic pyruvate cannot be responsible for the great difference in the inhibition pattern of tissue and mitochondrial respiration.

Second, the inhibitor concentration inside the cells might be lower than that outside, since amytal is a weak acid with a pK higher than 7.5 which can be unequally distributed among intra- and extracellular compartments due to a pH difference across the sarcolemma (0.2–0.3 pH units) [42]. If the protonated form of amytal possesses a higher permeability than the deprotonated (anionic) one, the concentration of the former inside the cell should be the same as that outside. As the intracellular pH is lower than the interstitial pH, the cytoplasmic concentration of the anionic form should be lower, so that the total concentration of amytal also should be lower and can be about 80% of the perfusate concentration. Hence, the large difference in the sensitivity to amytal inhibition of respiration of isolated mitochondria and perfused heart cannot be ascribed to reduced intracellular inhibitor concentration.

Thus, the discrepancy between the inhibitory curves in the aforementioned cases can, at least partially, reflect a significant control of cardiac respiration exerted by ADP and/or P_i via AN translocase, P_i carrier and ATP synthase under physiological conditions of high [ATP]/[ADP] ratio.

The control strength of NADH-CoQ reductase was roughly estimated in this paper to be equal 0.35. However, we have to bear in mind that this value is not very accurate for several reasons. First, the degree of inhibition of ADP-stimulated respiration of isolated mitochondria was taken as a measure of inactive NADH-CoQ reductase complexes. Obviously, the true content of inactive complexes should be lower and, therefore, the control strength is overestimated. Second, progressive enhancement of the [NADH]/[NAD^+] ratio due to an increasing suppression of NADH-CoQ reductase counteracts inhibition and, therefore, may decrease the apparent control strength. Third, in contrast, elevation of cytosolic [ADP] and [P_i] induced by amytal may shift control from AN translocase and P_i carrier to Complex I and increase the apparent control strength of the latter. In addition, a decrease in [ATP]/[ADP] ratio in matrix should activate PDH, ICDH and OGDH [23], increasing [NADH]/[NAD^+]. In other words, the apparent control strength is a variable parameter dependent on the metabolites listed above.

In addition to simple substrate regulation ([ADP], [P_i], [NADH], [O_2]), modulation of kinetic properties of particular enzymes and enzyme systems (maximal rates and K_m) could occur [23,30,31,43–45]. In the latter case Ca^{2+} is supposed to be the most possible modulator of kinetic parameters. Besides of activation of PDH, ICDH and OGDH [23,30,31], its influence on mitochondrial ATP synthase is suggested [43]. Also, the membrane potential may affect both kinetic properties of membrane-bound enzymes [23,44,45] and the intramitochondrial [ATP]/[ADP] ratio [40]. Furthermore, even elevation of uncoupled electron flux due to a rise of the [NADH]/[NAD^+] ratio resulted in an increase in the pseudo-first-order rate constants of cytochrome interaction in submitochondrial particles [45]. Finally, compartmentation of adenine nucleotides as well as other metabolites [23,24] may be involved in the integration of ATP formation and utilization.

Relationships between cardiac contractile function and cytosolic phosphates

Amytal-induced decline both in cardiac work index (PRP) and V_{O_2} was linked to the elevation of cytosolic [ADP] and [P_i] (Fig. 7) as well as to a decrease in [ATP]/[ADP] ratio and A(ATP). There are numerous works [8–17,20–22,46–50] where the influence of the aforementioned metabolites on contraction have been discussed. Among the proposed mechanisms there are inhibition of actomyosin ATPase activity by ADP and P_i [49] followed by reduction of maximal force and relaxation rate [48] as well as a decrease in the Ca^{2+} sensitivity of myofibrils by P_i [46,47]. It should be noted that, unlike hypoxia or anoxia [42,50], the inhibition of mitochondrial ATP production by amytal did not cause

acidosis at all (see also Ref. 14). Moreover, we have even found a slight alkalization of the intracellular medium induced by amytal at moderate coronary flows (see also Ref. 14). For this reason a pH decrease can be excluded from consideration as potential inhibitory factor.

In addition, all the aforementioned effects of increased [ADP] and [P_i] on PRP, EDP and velocities of contraction and relaxation can be mediated via Ca^{2+} turnover since the latter is ATP-dependent [51]. Hence, elevation of [ADP] and [P_i] may result in a decrease in systolic Ca^{2+} concentration and an increase in the diastolic one [21,52,53] and, therefore, in a depression of LVSP and rise in EDP. In fact, it has been recently found that the increase in EDP induced by anoxia was related to the elevation of diastolic [Ca^{2+}] [53]. An involvement of Ca ions in the regulation of energy turnover may be especially important in the experiments with isoproterenol. Actually, hearts exhibited significantly higher PRP values in the presence of Iso at the same magnitudes of [ADP] and [P_i], (Fig. 7A,B), i.e., performed equal work at much higher [ADP] and [P_i] and at much lower [ATP]/[ADP] and A(ATP). Also, a significantly lower end (and minimal) LV diastolic pressure was observed for the same values of metabolic indexes (Fig. 7C,D). This phenomenon may be explained by higher rate of Ca^{2+} turnover (HR elevation, Fig. 2B) as well as higher systolic (LVSP increase) and lower diastolic Ca^{2+} concentrations combined with reduced sensitivity of myofibrils to Ca^{2+} in the presence of Iso. All these factors overcome the unfavorable influence of elevated [ADP] and [P_i] as well as reduced [ATP]/[ADP] and A(ATP).

In this connection it is interesting to consider the effect of coronary flow on cardiac energy turnover, as it can be related in part to Ca^{2+} turnover. In fact, besides possible 'garden hose effect' (Refs. 54,55; however, see Ref. 13) and enhanced oxygen delivery [13], a distinct elevation of systolic Ca^{2+} [56] has been found to take place in response to the increase in coronary flow. However, in this case coronary flow-induced augmentation of PRP and V_{O_2} was not associated with alterations in cytosolic phosphates (Table I and Refs. 12,13,16) implying a precise coordination of respiration and mechanical function which is provided by the operation of a whole network of control mechanisms [23]. Note that PCr and P_i remained constant even after a decrease in coronary flow and perfusion pressure to values much lower than those used in this work [12,13,16]. The increase in amytal concentration above 0.5 mM was followed by a decline in both absolute and relative magnitude of PRP rise in response to coronary flow elevation (see Fig. 3B); ADP and P_i levels were not markedly affected by coronary flow at each inhibitor concentration (see Fig. 5). This implies that amytal somehow suppresses the operation of the mechanisms responsible for the link between energy turnover and coronary flow.

Dissociation between PRP and V_{O_2} induced by amytal (see Fig. 3), observed earlier in hypoxia [50], can be ascribed to other energy-consuming processes, the relative contribution of which to the total energy utilization increases. Hence, the efficiency of energy use for mechanical work expressed as, PRP/V_{O_2} ratio reduced 2.5-times as the amytal concentration increased (Fig. 3, inset). It can be related to several factors: (1) decrease in thermodynamic efficiency of energy utilization due to a fall in A(ATP); (2) energy expenditure for maintenance of ionic homeostasis and elevated diastolic pressure; (3) activation of energy dissipation via futile cycles and due to uncoupling of oxidative phosphorylation. However, the latter seems unlikely, since amytal is not an uncoupler in this concentration range.

Comparison of the effects of inhibition of the respiratory chain and energy transfer

There is a significant similarity between the physiological and biochemical consequences of the action of amytal [8,10] and graded hypoxia [15,42,50], amytal and iodoacetamide (IAAm) which inhibits cardiac creatine kinase [22,28]. In fact, blocking the respiratory chain at the level of NADH-CoQ reductase or cytochrome c oxidase (due to oxygen deficiency) results in a significant drop of cytosolic A(ATP) by 7 and 7 to 13 kJ/mol [15], respectively, and in a concomitant depression of PRP or systolic pressure [15] which is analogous to PRP at a fixed heart rate. However, in hypoxia $+dP/dt_m$ and $-dP/dt_m$ were less sensitive to a decline in A(ATP) as compared with systolic pressure; $-dP/dt_m$ did not fall starting from a certain reduced value of A(ATP) [15]. In contrast, in our experiments $+dP/dt_m$ was linearly related to the developed pressure throughout the complete range of inhibitor concentrations and coronary flows. Furthermore, the course of $-dP/dt_m$ as a function of $-\Delta G$(ATP) was different when induced by amytal and hypoxia. Such different behavior can be ascribed in part to moderate acidosis (0.2–0.3 pH units) which takes place during hypoxia [42,50] and is absent while amytal blocks electron transfer in the presence of pyruvate, lactate or acetate [14]. Furthermore, the difference in redox state of cytochromes, which should be more reduced in anoxia and more oxidized in the presence of amytal, should be taken into account.

Abolition of energy transfer through the PCr shuttle by IAAm also reduced maximal PRP and V_{O_2} values; however, the maximal amplitude of this effect did not exceed 40% [22,28]. It was associated with enhancement of EDP, concentrations of ADP and P_i as well as with a parallel decline in [ATP]/[ADP] and A(ATP) [22,28]. In this case all these events were due to the inhibition of the PCr shuttle that required acceleration

of energy transfer through the adenylate pathway and, hence, a rise in cytosolic [ADP]. Unlike respiratory chain inhibition, IAAm treatment did not cause an imbalance between energy supply and demand.

In all cases discussed above, changes in cytosolic [ADP] were closely related to those in [P_i]. Therefore, it is hard to resolve the effects of these metabolites. However, there is a model where alterations in [ADP] occurred at nearly constant P_i concentrations [14, 22,26,28]. It was achieved by using 2-deoxyglucose (DG) in the presence of pyruvate [22,26,28] or acetate [14]; the former reversibly trapped phosphate, reduced PRP and cytosolic [ATP]/[ADP] ratio without appreciable changes in [P_i]. Subsequent washout of DG was followed by a parallel recovery of PRP and [ATP]/[ADP] and decrease in [ADP] at constant [ATP] and [P_i] [22,26,28]. Consequently, cytosolic [ADP] can be considered as a potential regulator of contractile function.

Conclusions

We may thus, conclude that when energy turnover is controlled predominantly at the sites located in mitochondria (amytal inhibition, hypoxia), cytosolic [ADP], [P_i], [ATP]/[ADP] and ΔG(ATP) may provide a feedback between oxidative phosphorylation and contractile function. However, this type of control is not unique under these conditions and other control mechanisms also have to operate in order to facilitate a fine tuning of supply to demand. It can be Ca^{2+} modulation of dehydrogenases of the Krebs cycle [23,30,31]. In contrast, while energy turnover was activated by an increased coronary flow, a multi-site control mechanism equally varying supply and demand capacities probably operated. Again, it could be parallel, simultaneous Ca^{2+} regulation of contractile apparatus and mitochondria. Energy dissipation seems to be increased as A(ATP) reduced by amytal or IAAm action [22,28] and, consequently, may considerably affect coordination of mitochondrial energy production and myofibrillar energy utilization.

Appendix

Possible artifacts in measurements of phosphate metabolites in perfused heart

The major artifact arises from unequal load of the left and right ventricles of perfused heart; the latter remains unloaded. For this reason average concentrations of metabolites determined in the whole heart are the weighed sum of respective concentrations in the left and right ventricles (mass ratio approx. 4:1; atria can be neglected) which can be different because of the difference in the loads. This refers mostly to PCr and P_i concentrations and free [ADP] and ΔG(ATP) derived from them, since they are often workload-dependent unlike [ATP] which is stable under steady-state conditions. The situation is simple when alterations in cardiac work are not related to changes in observed concentrations of these metabolites as in our experiments where cardiac work has been varied by coronary flow. However, when reduction of PRP and V_{O_2} was induced by amytal, the dependence of [PCr] and [P_i] on amytal concentration may be different for unloaded right and loaded left ventricles. In the extreme case we may suppose that right ventricular PCr and P_i are not affected by amytal at all and observed concentrations are:

$$[C]_{obs} = 0.8[C]_L + 0.2[C]_R,$$

where $[C]_L$ and $[C]_R$ are concentrations in the left and right ventricles, respectively. In the absence of the inhibitor $[C]_L$ and $[C]_R$ should be approximately equal ($[C]_0$) and therefore:

$$[C]^0_{obs} = [C]^0_L = [C]^0_R$$

In the presence of amytal

$$[C]_{obs} = O.8[C]_L + O.2[C]_R$$

If for PCr at maximal concentration of amytal

$$[C]_{obs} = 0.5[C]^0_{obs} \text{ (see Fig. 5)}$$

then $[C]_L = 0.375[C]_{obs}$, i.e., the true concentration of PCr in the left ventricle is lower than the observable one by 25% or by 12.5% with respect to the initial ($[C]^0_{obs}$). In turn, the maximal error in the estimation of [ATP]/[ADP] ratio and [ADP] is about 30%; true values of the former are lower and those of the latter are higher. However, it is hardly possible that the PCr concentration in the unloaded right ventricle was not affected by amytal at all. A certain decrease of PCr, though less significant than in the left ventricle, seems to occur. Therefore, respective systematic errors should be less significant than those given above for the extreme case.

A similar situation occurs for [P_i] estimation. If at maximal [amytal] for P_i $[C]_{obs} = 3[C]^0_{obs}$ (see Fig. 5), then $[C]_L = 3.5[C]^0_{obs}$, i.e., true [P_i] in the left ventricle is higher than the observed one by approx. 17%. Accordingly, the true $-\Delta G$(ATP) value should be lower by 0.4 kJ/mol due to higher [P_i] and totally including the effect of reduced [ATP]/[ADP] ratio by 1.4 kJ/mol. Again, the same arguments as for PCr in favor of lower real magnitude of systematic errors are applicable for [P_i]. However, there is an additional potential source of systematic errors in the [P_i] determination which has been pointed out by Allen et al. [57]. Briefly, manipulation with the heart before perfusion may lead to damage of some amount of cardiomyocytes in which PCr can be completely splitted to Cr and P_i. Taking the

amount of such cells to be equal to 5% of total and [PCr]/[P_i] ratio from 3 to 6 we find that the increment of P_i is between 15 and 30% of the true value. Therefore, the P_i concentration observed in normal heart can be somewhat overestimated, maximally by 15–30%. Progressive increase in P_i concentration induced by the increasing in amytal concentration will significantly reduce contribution of this systematic error to 5–10% because of, at least, a 3-fold elevation in [P_i].

NMR technique allows to determine free concentrations of some metabolites which are in different cellular compartments, e.g., in mitochondria and cytoplasm. P_i which is seen in the ^{31}P-spectra of normal heart as a single peak at approx. 4.95 ppm downfield of the PCr peak belongs to the cytoplasmic pool of P_i since its chemical shift corresponds to pH 7.1–7.2 [58], characteristic for cytosol. Mitochondrial P_i which should have a peak located between the phosphomonoesters and cytosolic P_i peaks (0.5 ppm downfield of the cytosolic P_i peak) in accordance with a more alkaline intramitochondrial medium (by about 0.5 pH units [59]) is usually not seen in the spectrum. Therefore, [P_i] values obtained by ^{31}P-NMR in our experiments are referred rather to cytosolic P_i. Unlike P_i, ATP, which is present predominantly in the form of MgATP, has the same chemical shift even for the Beta-P peak most sensitive to the environment in the myoplasm and mitochondrial matrix [58]. Therefore, cytosolic ATP was taken to be equal to 85% of the total assuming 15% pool size of mitochondrial ATP (see Materials and Methods). If mitochondrial ATP is not NMR-visible then cytosolic [ATP] and [ADP] have been underestimated by 15% whereas cytosolic [ATP]/[ADP] ratio and ΔG(ATP) are independent of adenine nucleotide distribution.

Thus, possible systematic errors in the determination of cytosolic [ATP], [ADP], [P_i], [ATP]/[ADP] and ΔG(ATP) are essentially smaller than the amplitude of their changes and, therefore, do not significantly distort pattern the of the changes in these parameters in our experiments.

Acknowledgements

The authors are very grateful to Prof. V.A. Saks for constant attention to this work and helpful and stimulating discussions.

References

1 Opie, L.H. (1965) J. Physiol. 180, 529–541.
2 Neely, J.R, Liebmeister, H. and Morgan, H. (1967) Am. J. Physiol. 212, 815–822.
3 Williamson, J.R., Ford, C., Kobayashi, K., Illingworth, J. and Safer, B. (1976) Circ. Res. 38(suppl. 1), 39–48.
4 Chance, B. and Williams, G.R. (1955) J. Biol. Chem. 217, 385–393.
5 Klingenberg, M. (1961) Biochem Z. 335, 263–272.
6 Slater, E.C. (1973) Biochim. Biophys. Acta 292, 543–553.
7 Erecinska, M., Wilson, D.F. and Nishiki, K. (1978) Am. J. Physiol. 234, C82–C89.
8 Nishiki, K., Erecinska, M. and Wilson, D.F. (1979) Am. J. Physiol. 237, C221–C230.
9 Geisen, J. and Kammermeier, H. (1980), J. Mol. Cell. Cardiol. 12, 891–907.
10 Nuutinen, E.M., Nishiki, K., Erecinska, M. and Wilson, D.F. (1982) Am. J. Physiol. 243, H159–H169.
11 Kammermeier, H., Schmidt, P. and Jungling, E. (1982) J. Mol. Cell. Cardiol. 14, 267–277.
12 Clarke, K. and Willis, R.G. (1987) J. Mol. Cell. Cardiol. 19, 1153–1160.
13 Marshall, R.G. (1987) J. Clin. Invest. 82, 86–95.
14 Hoerter, J., Lauer, C., Vassort, G. and Gueron, M. (1988) Am. J. Physiol. 255, C192–C201.
15 Griese, M. Perlitz, V., Jungling, E. and Kammermeier, H. (1988) J. Mol. Cell. Cardiol. 20, 1189–1201.
16 Weiss, R.G., Chacko, V.P., Glickson, J.D. and Gerstenblith, G. (1989) Proc. Natl. Acad. Sci. USA 86, 6426–6430.
17 From, A.H.L., Zimmer, S.D., Mishursky, S.P., Mohanakrishnan, P., Ulstad, V.K., Thoma, W.J. and Ugurbil, K. (1990) Biochemistry 29, 3731–3743.
18 Jacobus, W.E. (1985) Annu. Rev. Physiol. 47, 707–725.
19 Hassinen I.E. (1985) Biochim. Biophys. Acta 853, 135–151.
20 Gibbs, C. (1985) J. Mol. Cell. Cardiol. 17, 727–731.
21 Allen, D.G. and Orchard, C.H. (1987) Circ. Res. 60, 153–168.
22 Kupriyanov, V.V., Lakomkin, V.L., Kapelko, V.I. and Saks, V.A. (1990) Biomed. Sci. 1, 4–12.
23 Heineman, F.W. and Balaban, R.S. (1990) Annu. Rev. Physiol. 52, 523–542.
24 Saks, V.A., Rosenshtraukh, L.V., Smirnov, V.N. and Chazov, E.I. (1978) Can. J. Physiol. Pharmacol. 56, 691–706.
25 Kupriyanov, V.V., Steinschneider, A.Ya., Ruuge, E.K., Kapelko, V.I., Zueva, M.Yu., Lakomkin, V.L., Smirnov, V.N. and Saks, V.A. (1984) Biochim. Biophys. Acta 805, 319–331.
26 Kupriyanov, V.V., Lakomkin, V.L., Kapelko, V.I., Steinschneider, A.Ya., Ruuge, E.K. and Saks, V.A. (1987) J. Mol. Cell. Cardiol. 19, 729–740.
27 Kapelko, V.I., Kupriyanov, V.V., Novikova N.A., Lakomkin, V.L., Steinschneider, A.Ya., Severina, M.Yu., Veksler, V.I. and Saks, V.A. (1988) J. Mol. Cell. Cardiol. 20, 465–479.
28 Kupriyanov, V.V., Lakomkin, V.L., Steinschneider, A.Ya., Novikova, N.A., Saks, V.A. and Kapelko, V.I. (1989) in Pathophysiology and Pharmacology of Heart Desease (Anand, I.S., Wahi, P.L. and Dhalla, N.S., eds.), pp. 45–86, Kluwer, Boston.
29 Steenbergen, C., Deleeuw, G. and Williamson, J.R. (1978) J. Mol. Cell. Cardiol. 10, 617–639.
30 Denton, R.M. and McCormack, J.G. (1980) FEBS Lett. 119, 1–8.
31 Hansford, R.G. (1985) Rev. Physiol. Biochem. Pharmacol. 102, 1–62.
32 Katz, L.A., Koretsky, A.P. and Balaban, R.S. (1987) FEBS Lett. 221, 270–276.
33 Katz, L.A., Koretsky, A.P. and Balaban, R.S. (1988) Am. J. Physiol. 255, H185–H188.
34 Saks, V.A., Chernousova, G.B., Gukovsky, D.E., Smirnov, V.N. and Chazov, E.I. (1975) Eur.J. Biochem. 57, 273–290.
35 Bergmeyer, H.U. (1974) Methods in Enzymatic Analysis. 2nd Edn., pp. 1625–2305, Academic Press, New York.
36 Eggleton, P. Elsden, S.L. and, Gough, N. (1943) Biochem. J. 337, 526–529.
37 Lawson, J.W.R. and Veech, R.L. (1979) J. Biol. Chem. 254, 6528–6537.
38 Bunger, R. and Soboll, S. (1986) Eur. J. Biochem. 159, 203–213.
39 LaNoue, K.F., Bryla, J. and Williamson, J.R. (1972) J. Biol. Chem. 247, 667–674.
40 Tager, J.M., Wanders, R.G.A., Groen, A.K., Kunz, W., Bohnen-

sack, R., Kuster, U., Letko, J., Bohme, G., Duszynski, J. and Wojtszak, L. (1983) FEBS Lett. 151, 1–9.
41 Kascer, H. and Burns, J.A. (1979) Biochem. Soc. Trans. 7, 1149–1160.
42 Kusuoka, H., Weisfeldt, M.L., Zweier, J.L., Jacobus, W.E. and Marban, E. (1986) Circ. Res. 59, 270–282.
43 Das, A.M. and Harris, D.A. (1990) Cardiovasc. Res. 24, 411–417.
44 LaNoue, K.F., Jeffris, F.M. and Radda, G.K. (1986) Biochemistry 25, 7667–7675.
45 Saks, V.A., Kupriyanov, V.V. and Luzikov, V.N. (1972) Biochim. Biophys. Acta 283, 42–53.
46 Kentish, J.C. (1986) J. Physiol. (Lond.) 370, 585–604.
47 Mekhfi, H. and Ventura-Clapier, R. (1988) Pflügers Arch., 411, 378–385.
48 Schoenberg, M. and Eisenberg, E. (1987) J. Gen. Physiol. 89, 905–920.
49 Sleep, J. and Glyn, H. (1986) Biochemistry 25, 1149–1154.
50 Mathews, P.M., Talor, D.J. and Radda, G.K. (1986) Cardiovasc. Res. 20, 13–19.
51 Sperelakis, N. and Schneider, J.A. (1976) Am. J. Cardiol. 37, 1079–1085.
52 Lee, J.A. and Allen, D.J. (1988) Pflügers Arch. 413, 83–89.
53 Kihara, Y., Grossman, W. and Morgan, J.P. (1989) Circ. Res. 65, 1029–1044.
54 Arnold, G.F., Kosche, E., Meissner, E., Neitzert, A. and Lochner, W. (1968) Pflügers Arch. 299, 339–356.
55 Miller, W.P., Shimamoto, N., Nellis, S.H. and Liedtke, A.J. (1987) Am. J. Physiol. 253, H1271–H1278.
56 Marban, E., Kitakaze, M., Chako, V.P. and Pike, M. (1988) Circ. Res. 63, 673–678.
57 Allen, D.J., Eisner, D.A., Morris, P.G., Pirolo, J.S. and Smith, J.L. (1986) J. Physiol. (Lond.) 376, 121–141.
58 Ingwall, J.S. (1982) Am. J. Physiol. 242, 472–744.
59 Williamson, J.R. (1979) Annu. Rev. Physiol. 41, 485–506.